Visión Electrónica

Más que un estado sólido

https://revistas.udistrital.edu.co/index.php/visele
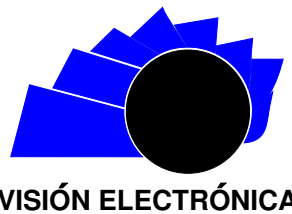
UNIVERSIDAD DISTRITAL FRANCISCO JOSÉ DE CALDAS

VISIÓN ELECTRÓNICA

A RESEARCH VISION

Design of a magnetic encoder using the Hall effect

Diseño de un encoder magnético usando efecto Hall

William Alejandro López-Contreras [ID][1], *José Danilo Rairán-Antolines* [ID][2]

ABSTRACT

We present the design of a magnetic encoder for angular position measurements. The proposed encoder includes two Hall sensors in quadrature in a fixed platform. In addition, two permanent magnets are placed above the sensors in a shaft. The relative motion between the fixed and movable components generates a voltage variation in the sensors, which enables an approximation of the angular position. We detail the acquisition process and the linearisation method applied for this encoder, which represent the most important contributions of this work. Finally, we demonstrate an application of the encoder for position control of a direct current motor to characterise the encoder performance in estimating rapid and slow changes in angular position.

RESUMEN

En este artículo se presenta el diseño de un encoder magnético para la medición de la posición angular. El encoder está compuesto por dos sensores de efecto Hall en cuadratura en una plataforma fija. Además, sobre los sensores, y en el eje a medir se ubican dos imanes permanentes con magnetización axial. El movimiento relativo entre el componente fijo y el móvil del encoder genera una variación de voltaje en los sensores. Esta variación da lugar a la aproximación de la posición angular. Se detallan los procesos de adquisición y linealización de los datos, dado que son los aportes más importantes de esta propuesta. Para finalizar se muestra la aplicación del encoder en el control de posición angular del eje de un motor de corriente directa, con lo que se muestra el trabajo del encoder ante cambios lentos y rápidos de posición.

[1]Electronic Technologist, Universidad Distrital Francisco José de Caldas, Colombia. E-mail: gice@udistrital.edu.co.
[2]BSc in Electric Engineering, MSc in Industrial Automation, Ph.D. in Engineering - Systems and Computing, Universidad Nacional de Colombia, Colombia. Current position: Professor at Universidad Distrital Francisco José de Caldas, Colombia. E-mail: drairan@udistrital.edu.co

1.   Introduction

To improve industrial processes, the physical phenomena related to magnetism are currently a subject of study for the design of current sensors [1], magnetic field sensors [2] and position sensors [3–5]. An important goal of these studies is to improve sensor characteristics such as precision, resolution and sensitivity. The operating principle of these sensors is based on changes in a magnetic field due to the Hall effect, as reported in [6, 7], or the magnetoresistive effect, as described in [8]. In addition, to improve the quality of these sensors, numerous methods and algorithms have been studied to compensate for errors. In particular, position measurements include aspects such as 1) geometric orientation, as in [9], 2) polarity and magnetic materials, as in [10, 11] and 3) the position of the sensor itself, as in [12]. Once the sensor measurements are obtained, the output of the sensor should be linearised. This linearisation process can be performed by using artificial neural networks, as in [9] and [13], running polynomial approximations, as in [14], or applying other methods, such as the approached described in [15].

Numerous industrial fields, such as robotics, biomedicine, commuting and defence, require the measurement of angular position. Due to the broad range of possible applications, improvements are desired in the current measurement technology, such as the proposals in [16,17]. Current studies have focused on the design and construction of encoders, which, in addition to improving the performance, precision, sensitivity, resolution and response time, should be robust under extreme weather conditions without a degradation in the estimation quality, as presented in [18].

Among the conventional methods for measuring angular position, the incremental encoder is the most popular. Therefore, this type of encoder has been studied over the past decades, which is one its primary advantages. However, the incremental encoder may present errors due to vibrations and pollution. This sensor also presents errors when used in locations with gases or small remains of any material. Moreover, incremental encoders can require large areas for industrial applications, and their output is relative to the initial measurement, rather than being absolute, given that their primary component is a slotted disk.

In contrast to incremental encoders, magnetic encoders provide absolute measurements and are contactless, which guarantees high performance under various environmental conditions. Thus, this paper focuses on the development of an absolute magnetic encoder.

The remainder of this paper is organised as follows. Section 2 presents the operation of a magnetic encoder, and Section 3 describes its construction. Section 4 details the acquisition and signal processing. Section 5 presents an application of the fabricated sensor in controlling the angular position of a motor, and finally, Section 6 reports conclusions and future work.

2.   Operating Principle of the Sensor

The device presented in this paper estimates the angular position based on variations in a magnetic field resulting from the motion of two magnets with respect to a fixed position. The resultant field is measured by two Hall effect sensors located in quadrature. Thus, the voltage in the sensors generates a sine wave signal corresponding to the shaft angle to be measured. In general, the output voltage of the sensor is expressed as follows: $v_x = A\cos(\theta)$ and $v_y = B\sin(\theta)$, where θ is the rotation angle in radians, A and B are the signal amplitudes and v_x and v_y are the voltages in each sensor. Therefore, the approximations determined by the sensor are absolute for one turn, because each point in one revolution has a corresponding pair $\langle v_x, v_y \rangle$. Figure 1 presents the configuration of the magnets, denoted by their north (N) and south (S) magnetic polarity. The figure also shows the location of the Hall effect sensors.

Figure 1: Two Hall effect sensors in quadrature and a pair of magnets.
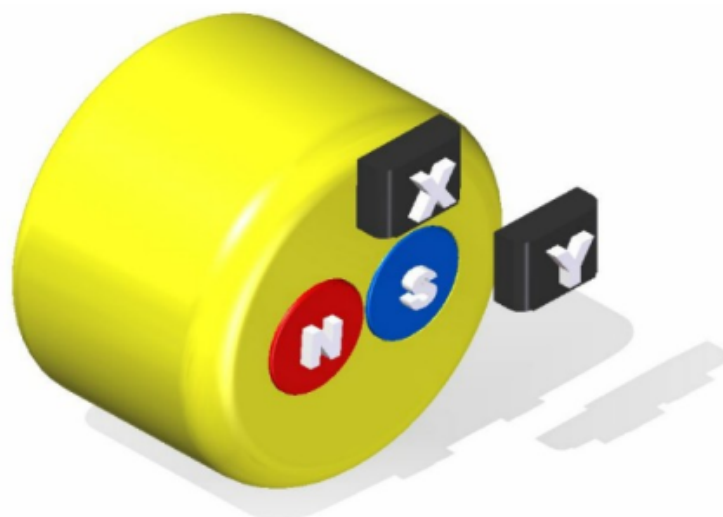
Source: own.

Given the configuration in Figure **1** and the outputs of the sensors, the angular position is obtained from Equation (**1**).

$$\theta = tan^{-1}\left(\frac{v_y}{v_x}\right) \tag{1}$$

3. Sensor Construction

An experimental procedure was applied to select the appropriate magnet for application, neodymium NdFeB. These magnets have a highly concentrated magnetic field, and their surfaces are smooth. The optimal distance between the magnets and sensors was experimentally determined as 10 mm. This distance produces voltage variations in the sensor with sufficient magnitude to obtain the maximal resolution for the analogue/digital converter, as will be described later.

The sensor for measuring variations in the magnetic field is a DRV-5053 sensor (Texas Instruments), which provides a source voltage range of 2.5–38 V. The sensor is thermally stable between -40° and 125° C, which is ideal for the application reported in this paper. The sensitivity of the sensor is + 45 mV/mT ± 10 % with respect to the temperature, which is sufficient for most industrial applications without sacrificing precision. However, if the temperature is a concern, the reader is referred to [18], which proposes a method for reducing the error caused by changes in the ambient temperature.

The sensor data are validated by using a protractor as a reference. In addition, the output of the sensor is compared with that of a goniometer. The protractor differentiates measurements in increments of 1°, as shown in Figure **2**.

Figure 2: Protractor and needle indicator.
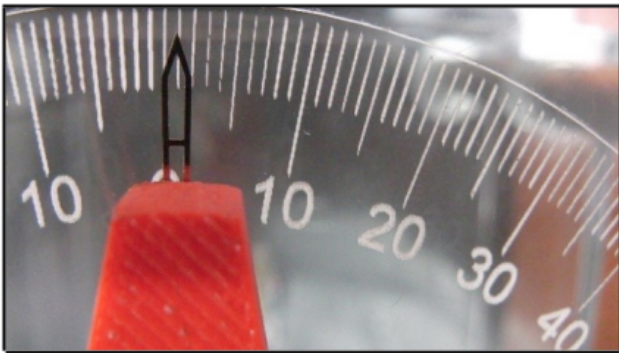
Source: own.

The needle indicates an angle, as shown in Figure **2**, which enables comparisons between the protractor measurement and the sensor output. The pointer has a needle at the end and a 3D prototyped piece that is attached to the shaft. The needle shape is particularly important for calibrating the sensor. Figure **3** shows the final prototype of the sensor.

Figure 3: Absolute and angular position measurement prototype.
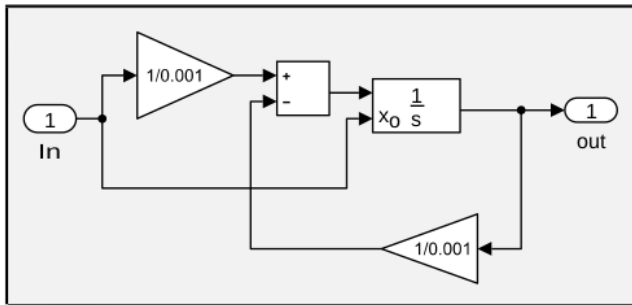

Source: own.

4. Data Acquisition and Signal Processing

The data acquisition is initiated as the sensor voltage is read using a PCI-6024E data acquisition card. This card has 12 bits of resolution and processes data at 200 kS/s with an adjustable input range of ± 10 V, ± 5 V, ± 1 V and ± 0.5 V.

First, the signal from the sensor is passed through a low-pass filter. With this filtering, the signal should present a good approximation of the sensor output because the first measurement is not initialised as zero, as is traditionally performed using transfer functions. Thus, we apply the process shown by the block diagram in Figure **4** rather than a traditional transfer function block. The configuration in Figure **4** sets the initial condition of the integral equal to the initial input, which avoids fluctuations around the true measurement that may cause instabilities for the control sensor. The first gain in

Figure **4** corresponds to the inverse of the constant time of the sensor, 1 ms. This constant time guarantees noise cancellation and normal operation of the sensor.

Figure 4: Low-pass filter to reduce noise effects.

Source: own.

Once the signal has been filtered, the X and Y signals are normalised. The normalisation eliminates any direct current (DC) components and sets the signal amplitude equal to 1. This process is performed by subtracting the mean value and then multiplying by the inverse of the maximum value. Figure **5** shows the normalisation results, where the sinusoidal nature of the signals becomes evident.

Figure 5: Sensor output, including an offset and amplitude adjustment.
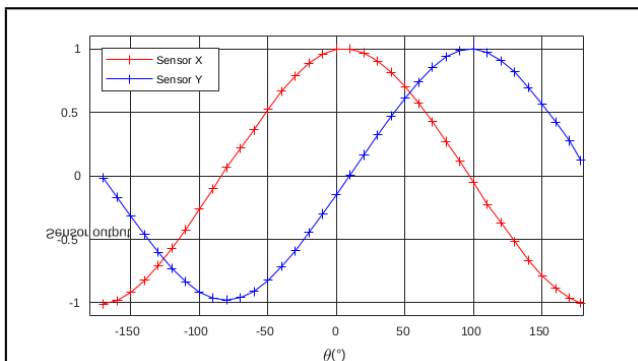
Source: own.

The signals in Figure **5** represent the inputs of the expression in Equation (**1**), which provides the estimated angle in radians. Then, the signal processing transforms the angle into degrees. The signal in degrees is input into a neural network to linearise the sensor output. However, prior to this step, an additional normalisation step is performed, in which the signal is divided by 100. This normalisation ensures that the sensor variations are close to 1, which is a general recommendation for

training neural networks.

The application of a neural network to linearise the measurement is indispensable given that the sensor estimations shown in Figure **5** may have errors exceeding 5°. This large error is partially due to the difficulty encountered in precisely locating the sensors and magnets in quadrature. The sensor design is based on a polynomial linearisation, but the error obtained with the neural network is lower. In particular, the neural network is a multilayer perceptron with one hidden layer. The network uses 'tansig' transfer functions for the input and hidden layers, while the transfer function of the output layer is linear.

The optimal neural network was selected via an experimental process. We tested combinations of 2–16 neurons in the input layer and 4–64 neurons in the hidden layer. To reduce the number of possible combinations, we tested only inputs of 2 to the power n, where n is an integer. In other words, 2, 4, 8 and 16 neuron were applied for the first layer, and 4, 8, 16, 32 and 64 neurons were applied for the second layer. The performance of the network improves as the number of neurons grows, but a high number of inputs also requires a high computation time. Therefore, the number of neurons for the inputs was set to 8, with 4 for the hidden layer.

The network output must be amplified 100 fold because the input was normalised by dividing by 100. Thus, the controller output has a range of ±180°. We applied an algorithm to extend the measurement range to any number of turns. This algorithm observes jumps that occur from -180° to 180° or vice versa and correspondingly subtracts or adds 360° to the estimation. Thus, the sensor output is smooth regardless of the number of turns. The application of this algorithm does not imply that the sensor is absolute for any number of turns; rather, the starting angle remains within a range of ±180°.

Figure **6** presents a block diagram of the sensor, including the previously described signal processing. The diagram includes the noise reduction, normalisation, angle computation, unit conversion, normalisation, linearisation, re-scaling and finally a jump avoidance algorithm.

Based on the prototype construction, we measured the error behaviour of the sensor, as shown in Figure **7**. The training stage for the neural network uses the mean squared error as a measure of performance. Figure **7** presents the results obtained by training 200 neural networks. The error for the best network is shown in the top panel of Figure **7**.

Figure 6: Block diagram of signal processing for the sensor.
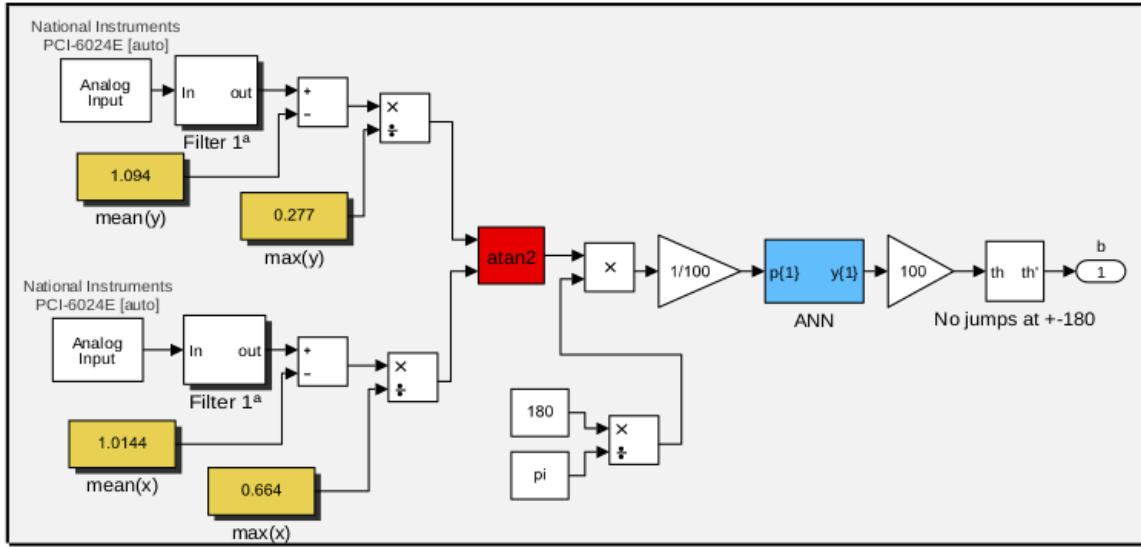
Figure 7: Neural network performance for 8 neurons in the first layer and 4 neuron in the second layer.
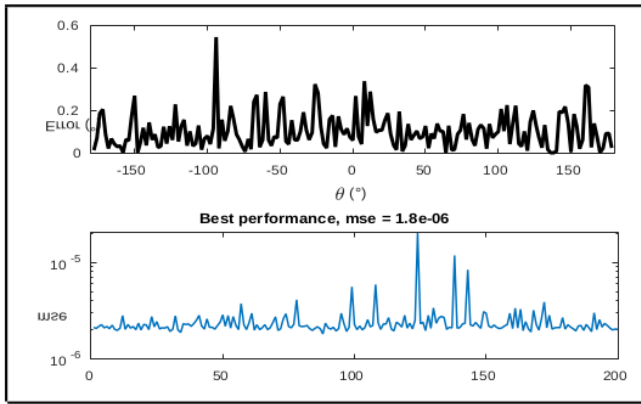
## 5. Application of the Encoder for Position Control of a Motor

The sensor was experimentally validated by controlling the angular position of a shaft, which is a traditional application for encoders. The experiment was performed to verify that the sensor properly measures the dynamic rotation of a shaft, in addition to the stationary measurement previously shown.

Let us consider a traditional PID controller with proportional, integral and derivative gains with respect to the error. In this controller, the proportional action serves to control plants that are already stable, but this type of controller may generate large steady-state errors. In contrast, the integral action (I) produces a controller output that is proportional to the accumulated error. This type of controller eliminates steady-state errors but slows down the system. Finally, the derivative action (D) predicts the behaviour of the error, which renders the control action faster. One disadvantage of the derivative component arises from noise amplification, which may make the system unstable. The union of these three actions (P+I+D) generates a better control action than the individual components. This combination is stable, eliminates steady-state errors, and is faster than the PI option. The final version of the controller is shown in Figure **8**, based on its implementation in Simulink.

The PID algorithm implemented in this system operates in the same manner as the controller reported in [17], but in this case, the nominal current is 500 mA. This current magnitude requires the implementation of a power amplifier, which maintains the actuating signal, u, according to the definition in Figure **8** and amplifies the current to the value required by the motor. The power amplifier allows changes in the sign of the actuating signal, which enables rotation control in both directions: clockwise and counter-clockwise. The amplifier is shown in Figure **9**. This power amplifier was built using LM386 operational amplifiers because these amplifiers use dual sources, which facilitates the connections of the circuit.

Figure 8: PID controller to regulate the position of a DC motor.
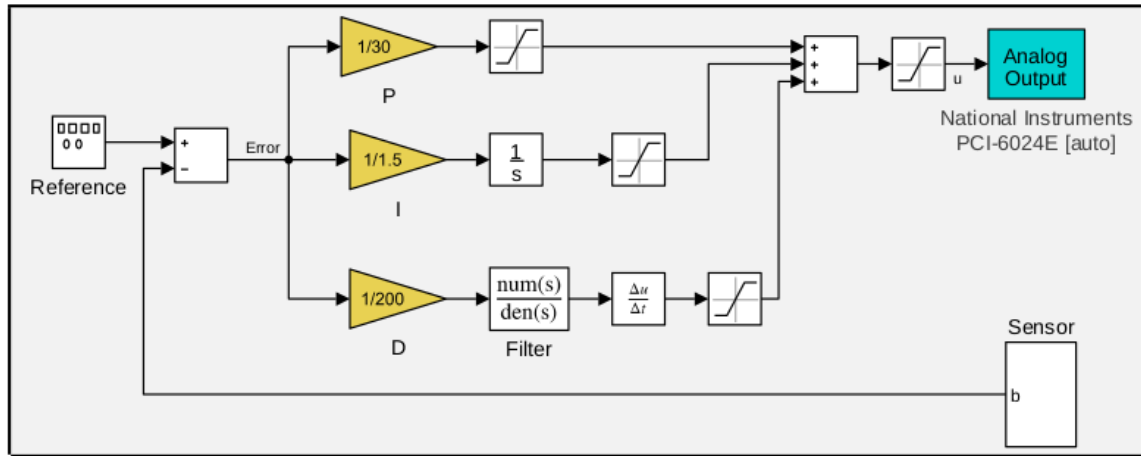
Source: own.

**Figure 9**: Power amplifier in a bridge configuration.
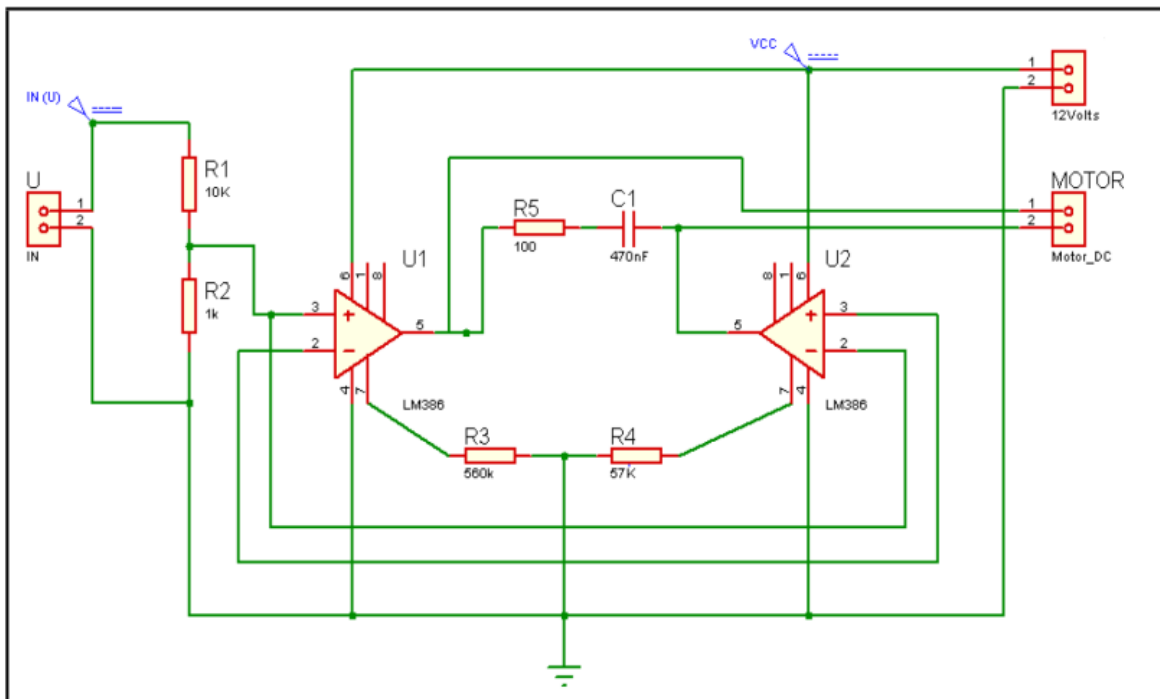
Source: own.

In the reported application, the motor must track a reference signal, r, using information from the designed encoder as a feedback signal. The motor properly tracks the reference signal, as shown in Figure 10. However, the behaviour observed between 2.5 and 3 s requires more attention. The controller does not have sufficient time to set the position of the shaft during this time period, and the output falls beneath the reference. This behaviour primarily arises from the dead zone. Due to this nonlinearity, the motor can only overcome the inertia and friction after reaching a threshold at which the integral of the controller accumulates a sufficient error to move the motor. The effect of the dead zone renders the control of this motor difficult, which is a consequence

of the motor design, rather than the building encoder.

Figure 10: Position control of a motor.
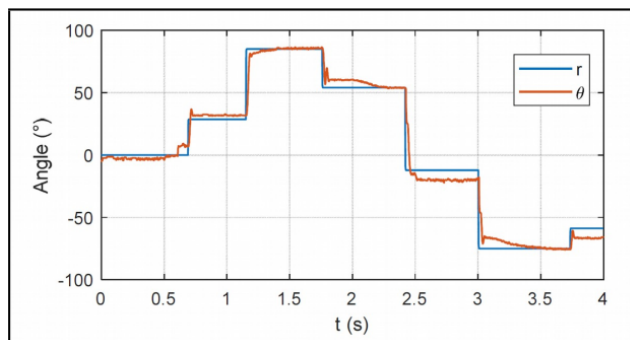
Source: own.

6.   Conclusions

In this paper, we presented the development of an absolute magnetic encoder based on two permanent magnets arranged in quadrature with axial magnetisation. The maximum error remains below 0.5° throughout the entire measurement range, which is equal to one turn. The utility of the designed measurement method was demonstrated with low cost and simple construction. The sensor was tested during the tracking of a reference signal corresponding to the angular rotation of a DC motor shaft.

To improve precision, sensitivity and resolution, studies should apply other methods for locating the sensor, as well as other magnetisation schemes, and should explore improvements in signal conditioning. In addition, it is important to increase the speed of data acquisition and the time response of the encoder. It would also be interesting to investigate other sensor configurations beyond a quadrature configuration.

References

[1] R. Weiss, R. Makuch, S. Member, A. Itzke and R. Weigel, "Crosstalk in Circular Arrays of Magnetic Sensors for Current Measurement," *IEEE Trans. Ind. Electron.*, vol. 64, no. 6, 2017, pp. 4903–4909. https://doi.org/10.1109/TIE.2017.2674630

[2] V. Luong, J. Jeng, B. Lai and C. Lu, "BT-01 Development of low-noise three-axis magnetometer with tunneling-magnetoresistance sensors," IEEE International Magnetics Conference (INTERMAG), Beijing, China, 2015. https://doi.org/10.1109/INTMAG.2015.7156761

[3] C. S. Anoop and B. George, "A new variable Reluctance-Hall Effect based angle sensor," Sixth International Conference on Sensing Technology (ICST), 2012. https://doi.org/10.1109/ICSensT.2012.6461720

[4] C. S. Anoop and B. George, "New signal conditioning circuit for MR angle transducers with full-circle range," *IEEE Trans. Instrum. Meas.*, vol. 62, no. 5, 2013, pp. 1308– 1317. https://doi.org/10.1109/TIM.2012.2236778

[5] S. Hao, Y. Liu and M. Hao, "Study on a Novel Absolute Magnetic Encoder," IEEE International Conference on Robotics and Biomimetics, Bangkok, Thailand, 2009, pp. 1773–1776. https://doi.org/10.1109/ROBIO.2009.4913270

[6] J. Liu, Z. Liu, Z. Wang and J. Cao, "AS5048 Magnetic Encoder for the Application in DC Motor Position Control of Portable Spectrometer," IEEE Advanced Information Management, Communicates, Electronic and Automation Control Conference, Xian, China, 2016, pp. 345–348. https://doi.org/10.1109/IMCEC.2016.7867230

[7] C. S. Anoop and B. George, "Study of a Hall Effect Brake Wear Sensor using Finite Element Modelling and Analysis," 19th Symposium IMEKO TC 4 Symposium and 17 th IWADC Workshop Advances in Instrumentation and Sensors Interoperability, Barcelona, Spain, 2013, pp. 480–484.

[8] B. George, V. J. Kumar and A. Chandrika Sreekantan, "Analysis of a tunneling magneto-resistance-based angle transducer," *IET Circuits, Devices Syst.*, vol. 8, no. 4, 2014, pp. 301–310.

[9] J. Kim and H. Son, "Two-DOF Orientation Measurement System for a Magnet with Single Magnetic Sensor and Neural Network," 14th International Conference on Ubiquitous Robots and Ambient Intelligence (URAI), 2017, pp. 448–453. https://doi.org/10.1109/URAI.2017.7992773

[10] Y. Liu, H. Hsiao and J. J. Chang, "Design and Validation of Polarity-Changeable Magnetizer for Encoding Patterns on Ring-Like Rotary Encoders," *IEEE Trans. Magn.*, vol. 53, no. 3, 2017, pp. 3–7. https://doi.org/10.1109/TMAG.2016.2626298

[11] S. Gauthier and D. M. Technologies, "The Development of a High Accuracy Multipole Strip Magnet for Non-Contact Linear and Rotary Position Measurement," *Dexter Magnetic Technologies Magazine*, 2012, pp. 1–9.

[12] S. Wu and Z. Wang, "Equilateral Measurement of Rotational Positions with Magnetic Encoders," *IEEE Trans. Instrum. Meas.*, vol. 65, no. 10, 2016, pp. 2360–2368. https://doi.org/10.1109/TIM.2016.2578579

[13] N. J. Medrano-Marques, B. Martin-del-Brio, A. Bono and C. Bernal-Ruiz, "Implementing Neural Networks onto Standard Low-Cost Microcontrollers for Sensor Signal Processing," IEEE Conference on Emerging Technologies and Factory Automation, vol. 2, 2005, pp. 967– 972. https://doi.org/10.1109/ETFA.2005.1612776

[14] J. Lara, S. Member, J. Xu and A. Chandra, "A Novel Algorithm Based on Polynomial Approximations for an Efficient Error Compensation of Magnetic Analog Encoders in PMSMs for EVs," *IEEE Trans. Ind. Electron.*, vol. 63, no. 6, 2016, pp. 3377–3388. https://doi.org/10.1109/TIE.2016.2524409

[15] M. Benammar, S. Member, A. Khattab and S. Member, "A Sinusoidal Encoder-to- Digital Converter Based on an Improved Tangent Method," *IEEE Sens. J.*, vol. 17, no. 16, 2017, pp. 5169–5179. https://doi.org/10.1109/JSEN.2017.2723619

[16] D. Rapos and C. Mechefske, "Dynamic Sensor Calibration: A Comparative Study of a Hall Effect Sensor and an Incremental Encoder for Measuring Shaft Rotational Position," IEEE International Conference on Prognostics and Health Management (ICPHM), 2016, pp. 1–5. https://doi.org/10.1109/ICPHM.2016.7542858

[17] J. D. Rairán-Antolines, C. E. Guerrero-Cifuentes and J. A. Mateus-Pineda, "PID and Fuzzy Controller Design for DC Motor Positioning," *Ingeniería y Universidad*, vol. 14, no. 1, 2010, pp. 137–160.

[18] X. Wang, H. Wang, H. Xie, D. Lou and K. Yang, "Design of Magnetic Encoder Based on Reconstructing and Mapping Looking-up Table," 19th International Conference on Electrical Machines and Systems (ICEMS), 2016, pp. 2–5.